

# Quantifying Power Distribution System Resiliency Using Code-Based Metric

Sayonsom Chanda, *Student Member, IEEE*, Anurag K. Srivastava<sup>✉</sup>, *Senior Member, IEEE*,  
Manish U. Mohanpurkar<sup>✉</sup>, *Member, IEEE*, and Rob Hovsapien, *Senior Member, IEEE*

**Abstract**—It is essential to improve the resiliency of power distribution systems (PDS) given the increase in extreme weather events, number of malicious threats, and consumers' need for higher reliability. This paper provides a formal approach to evaluate the operational resiliency of PDS and quantify the resiliency of a system using a code-based metric. A combination of steady state and dynamic simulation tools is used to determine the resiliency metric. Dynamic simulation tools help analyzing the impact of short-term events, which might affect operational resiliency in the long term. A dynamic optimization algorithm for changing operating criteria to increase the sustainability of the most critical loads has been proposed. The proposed theoretical approach is validated using a simple PDS model and simulation results demonstrate the ability to quantify the resiliency using the proposed code-based metric. The time-dependent quantification of resiliency has been demonstrated on a test system of two connected Consortium of Electric Reliability Technology Solutions (CERTS) microgrids.

**Index Terms**—Distributed energy resources, distribution systems, power system operations, renewable integration, resilience.

## I. INTRODUCTION

COMPLEX infrastructure networks, such as the electric power grid, are functional due to a number of factors, such as real time balance of generation and demand, automated control, complex human in the loop control, component-level availability, and system-level hierarchical interaction. Disruption of any scale at any hierarchical level can possibly threaten the continuity of the power grid services. Resilience of power distribution system (PDS) has gained significant traction after impact of super storm Sandy (2012) on the power grid reliability. However, inadequate theoretical foundations in the definition

and metrics relevant to PDS resilience challenge the practical implementation of resilience in electric utilities. PDS resilience is the ability of the network to resist discontinuity of power supply to critical loads during stressful operating conditions, and recover from any damages during the event [1]–[3]. PDS resilience metrics are important: 1) to justify investments in infrastructural upgrades for higher resilience; and 2) to evaluate the suitability of a particular approach to be taken by an operator to adequately enhance the resilience during a contingency or attack.

Threats to normal operations of PDS (i.e., power quality events, momentary interruptions, sustained outages, brownouts, and blackouts) are diverse, and have a wide range on the time scale (i.e., a time scale of milliseconds to several weeks). It is the objective of resilience-enabling efforts in PDS to maintain power supply to critical loads during emergencies, and maximize the time duration for which this supply can be maintained. Resilience metrics serve to capture the effectiveness of the strategy adopted to meet this objective of utilities. Several authors have proposed PDS resilience enhancements using networked microgrids [4], [5]. Technologies that augment advanced resource sharing between microgrids in anticipation of unfavorable events [6]–[8], or partitioning a PDS have also being actively researched and implemented across the industry [9], [10]. Several new improvements to control and operation of microgrids have been reported by researchers: such as resiliency-driven optimal scheduling [11], stochastic scheduling [12], and hierarchical outage management [13]. However, these approaches—though aimed at enhancing resilience—fall short of developing a tool in quantifying the resilience enhancements achieved by these technologies.

Resilience metrics developed from network topology can give us an approximate resiliency measure, but do not capture the availability of distributed energy resources to critical loads accurately in real time. The approach proposed in [15] requires exhaustive information about PDS infrastructure, and implicitly assumes infallibility of these resources during contingencies affecting a PDS. Physical infrastructure resources as well as state variables are susceptible to rapid and unforeseen changes [16]. Events in the distribution system, such as pole damage due to a car accident, sudden phase imbalance due to large current drawn by customers charging their electric vehicles, lightning strike, heavy rain followed by sudden drop in temperature, and transients due to variable power injections by photovoltaic generation connected to the power grid, voltage spikes, etc., affect the

Manuscript received May 15, 2017; revised August 12, 2017 and November 3, 2017; accepted December 23, 2017. Date of publication February 21, 2018; date of current version July 17, 2018. Paper 2017-IACC-0439.R2, presented at the 2016 IEEE International Conference on Power Electronics, Drives, and Energy Systems, Trivandrum, India, Dec. 14–17, and approved for publication in the IEEE TRANSACTIONS ON INDUSTRY APPLICATIONS by the Industrial Automation and Control Committee of the IEEE Industry Applications Society. This work was supported by the Idaho National Laboratory Directed Research and Development Program under the Department of Energy Idaho Operations Office under Contract DE-AC07-05ID14517. (Corresponding author: Anurag K. Srivastava.)

S. Chanda and A. K. Srivastava are with the School of Electrical Engineering and Computer Science, Washington State University, Pullman, WA 99163 USA (e-mail: sayon@ieee.org; asrivast@eecs.wsu.edu).

M. U. Mohanpurkar and R. Hovsapien are with Power and Energy Systems Department, Idaho National Laboratory, Idaho Falls, ID 83402 USA (e-mail: manish.mohanpurkar@inl.gov; rob.hovsapien@inl.gov).

Color versions of one or more of the figures in this paper are available online at <http://ieeexplore.ieee.org>.

Digital Object Identifier 10.1109/TIA.2018.2808483

resiliency of the network indirectly. Most PDS enable resiliency in response to an unfavorable event, and not in anticipation of an event. There are some approaches that emphasize on resilience-driven, adaptive restoration strategies [17], [18]. However, the approach is also not proactive and leverages a multimicrogrid approach, similar to [19] and [20]. Any reactive restoration approach results in system downtime, leading to financial losses, safety hazards, and public inconvenience [21]–[23]. There are several computation and data-related challenges to a prognostic approach of quantifying and enabling resilience, such as weather and consumer uncertainties, large meteorological data requirement, expense of processing that data, incorporating artificial intelligence to enable proactive response, and a lack of visibility into state parameters of the PDS [24].

We present an approach to quantify and monitor resiliency of PDS to an ongoing contingency, and proactively look ahead into the resiliency of the network to prolonged outages. The proposed approach enables the operator to have intuitive understanding into the long-term energy balance profile given the network's diverse backup energy resources and responsibility toward critical loads, without requiring detailed knowledge of the network model [25], [26]. Unlike a decision-theory based resiliency quantification tool [19], [27], the proposed method in this work quantify the resiliency of the network towards a broad range of possible scenarios instead of a singular predefined contingency addressed in other existing work.

The novel contributions of the paper compared to the existing work and building on our preliminary work are as follows [28].

- 1) The developed algorithm provides a time-dependent definition of resilience and a generic code-based framework for evaluating operational resilience of a PDS.
- 2) The developed algorithm demonstrates the use of a linear programming based dynamic optimization that can be adopted by utilities to maximize the resiliency of the most critical load following a contingency.
- 3) The developed algorithm can quantify and monitor resiliency in real time and proactively provide help in decision support to the PDS operator to maximize resiliency for broader range of possible contingencies and events.
- 4) The developed resilience does not require complete, low-level knowledge of the system infrastructure for computation, thus simple enough for operators to understand and use during contingencies.
- 5) The proposed approach makes a new contribution toward the development of a universal and easy to compare resiliency analysis metric for different distribution networks of variable sizes, capacity served, and critical priorities.

## II. TIME-DEPENDENT DEFINITION OF RESILIENCE

There are several working definitions of PDS resilience. Some authors have defined resilience as a function of the probability of attack and the consequence of that attack [29]. Resilience of PDS has also been defined based on the nature of attack on the system [23], [24], [30]. A framework to determine resilience based on the evaluation of infrastructure and the time taken to restore to service has been proposed in [16] and [31]. However, metrics based on inventory assumes that all resilience-enabling

infrastructures will operate during or after contingency, and cannot be used in real time. Cost metrics of damages incurred due to an attack has been commonly used to report a lack of resilience in the PDS [2]. The fundamental drawback of each of these definitions of resilience is that these definitions do not consider the durations of unfavorable events affecting the PDS. Consequently, the resilience metric derived using these definitions are meaningful only in the context of a specific attack, network topology, or data availability.

The importance of time to measure resilience of PDS has been discussed in detail in [16]. However, the inclusion of time as a factor of quantifying resilience is specific to one isolated event and the time taken to recover from that event. The network designer assumes that the system can be recovered after a certain amount of time. Power system events have a wide range of events. In practical scenario, the recovery time may vary greatly as the event progresses. In the proposed resilience metric, there is no such assumption. Using the he proposed algorithm, the resilience of the network can be computed for a wide time scale of events, ranging from a magnitude of  $10^0$  to  $10^6$  s, in a single computation step. Thus, using a single, easy-to-understand metric, the operator working through a contingency can be informed about the “service potential” of the network across a broad range of worst-case scenarios and optimize decision about seeking external resources to improve the operating condition of an affected distribution system or microgrid. Many resilience metrics proposed in the literature do not consider quantifying resilience across a wide-range of events in the power system considering duration of critical load affected. Thus, the proposed metric is novel contribution.

The proposed metric is derived from empirical equations that capture the impact of an unfavorable event to the network for a given time scale. The result of the equation is mapped to integer value between 1 and 10, representing low to high resiliency of the network for the assessed time scale. The same equation is used to evaluate the impact of events lasting from seconds to weeks. After all these computations are completed, the derived integral values are combined and represented as a single number. This single number representation is essentially a “code,” representing a state of resilience of the network, and does not correspond to any numerical value.

Conventionally, reliability metrics [such as system average interruption duration index (SAIDI), system average interruption frequency index (SAIFI), and momentary average interruption frequency index (MAIFI)] were adequate to describe the performance of a utility in providing service to consumers. Due to increase in the number of reported weather-based or human-induced physical events on the PDS [32], energy mix of renewable and conventional power sources, and cybersecurity breaches across the power grid [33], it has become indispensable to make the PDS resilient to these events/attacks. Though power system reliability and resilience are different concepts [20], they share an inherent dyadic relationship as metrics for evaluating system performance. Irrespective of the nature of the attack, the impact is best assessed by the time taken by a system to recover from the consequences of the attack. A time-domain mathematical formulation of resilience will facilitate mapping between the quantification of system performance by the two in-

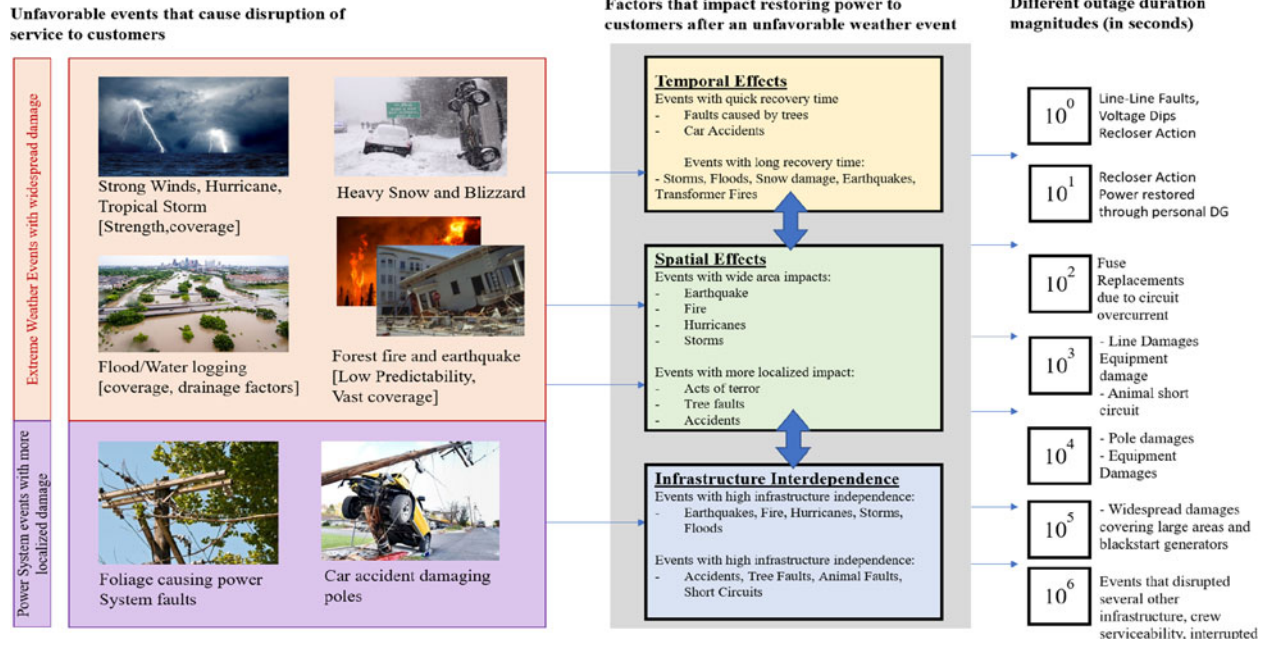


Fig. 1. Relationship between unfavorable weather events, and their spatio-temporal impacts and consequent power outage durations.

dependent concepts. Unfavorable events vary widely in terms of predictability, geographical coverage of the event, and the time left for preparation until the event happens eventually (such as in the case of hurricanes). Alongside state of the distribution system infrastructure, the impact of the event depends on the interdependence of infrastructures, and the spatial and temporal impacts of the unfavorable events, as shown in Fig. 1. Fig. 1 also shows the relationship between the diversity of events and the subsequent power outage duration.

There are several other desirable properties in a resilience metric.

- 1) The resilience metric (say  $R$ ) should be easily comprehensible and interpretable by operators, so that quick decisions can be made during ongoing contingencies.
- 2)  $R$  should be simple, robust, flexible, scalable, and applicable to any distribution system with minimal modification.
- 3) Computation of  $R$  should not exceed response time of distribution system control actions.
- 4) Interpretation of sensitivity of  $R$  should corroborate to physical changes in the network.
- 5) Attacks on the power system can disrupt both the quality and continuity of service, for varying durations of time. It is important for  $R$  to capture both attributes of the effect of the attack on the power system.  $R$  should preserve maximum information about all the noncommensurate factors that affect PDS resilience.
- 6)  $R$  must be characterized by low barrier to entry, easy to implement in distribution management systems (DMS), and compatible with existing and future data acquisition hardware. The format for  $R$  metric data exchanged should also follow common data exchange protocols.

Using [31], it can be deduced that PDS system interruptions follow a long-tailed distribution, and the impact of resilience

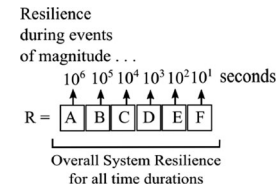


Fig. 2. Proposed resiliency metric.

inadequacy grows exponentially with outage duration. Thus, resilience of a PDS is a function of time duration of outage, as well as the number of loads that are affected by an outage event. In order to capture these two factors, let us propose that the resilience metric of a distribution system be represented as a coded numeric value, where  $A, B, \dots, F$  are all variables.  $R$  is defined as such in Fig. 2, since it is proportional to power outage duration and power outage magnitude. Each variable corresponds to a time scale of a power system event corresponding to the magnitude of its duration in seconds. Each variable in the definition of  $R$  in Fig. 2 represents the resilience of the system for corresponding duration of time outage in orders of 10.

The proposed approach considers such small time-scale events into resilience evaluation in order to accommodate transient power interruptions can stop or reset operations, leading to lost productivity for long outage durations. In context of resilience, we will consider the fraction of load ( $f$ ) *unaffected* by voltage or current distortion

$$f = \frac{\text{Load unaffected by PDS event (kW)}}{\text{Total load of PDS (kW)}} \quad (1)$$

where for events that disrupt power continuity in  $f$  fraction of load in the magnitude of  $10^0$  s, the resilience value is computed on an integer scale of 0 to 9, and stored in the variable  $F$ .



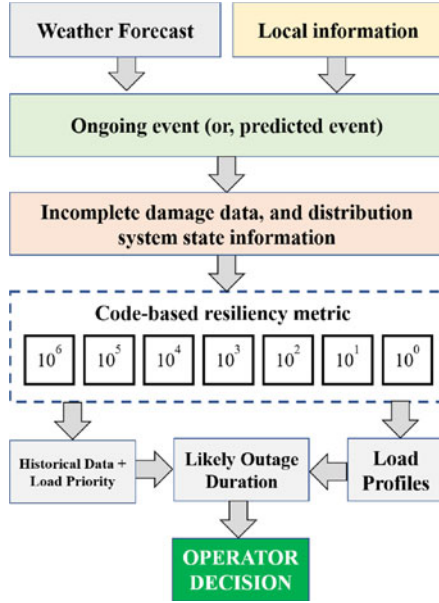


Fig. 3. Implementation of code-based resilience metric as a decision making tool for the operator.

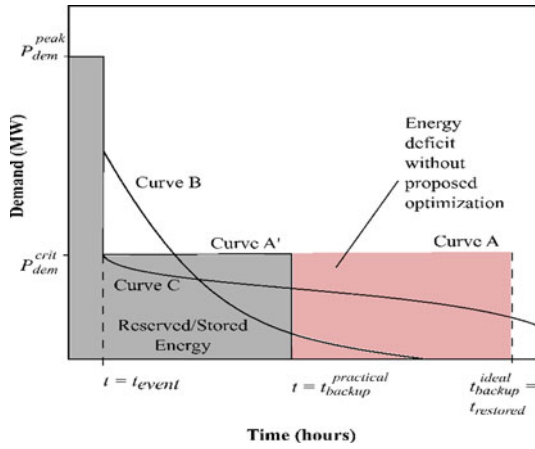


Fig. 4. Visual representation of energy deficit under different operation methods.

Similarly, for events lasting in the magnitude of minutes (i.e.,  $10^1$  s), the resilience value is computed on an integer scale of 0 to 9, and stored in the variable  $E$ , and so forth for variables  $D$ ,  $C$ ,  $B$ , and  $A$ .

#### A. Implementation of Code-Based Metric as an Industrial Tool

The code-based metric computes (based on last known state of the system, and other available data about resources) how likely the system is supply power to all its critical loads, on a scale of 1 to 9. In other words, considering a typical data flow, an unfavorable event is either forecasted to happen using weather forecasts or local intelligence, or the event happens with very short notice (as shown in Fig. 3). In both cases, the full impact is not known *a priori* or during the event. Since at the time of outage, the root cause of the outage is neither

TABLE I  
SCALING OF RESILIENCY METRICS

$m'$	1.00-3.71	3.72-6.42	6.43-9.13	9.14-11.85	11.86-14.56	14.57-17.27	17.28-19.98	19.99-22.71	22.71-25.41
$m$	1	2	3	4	5	6	7	8	9
	Low Resilience			Moderate Resilience				High Resilience	

clearly known, nor one can determine with certainty how long would the repair work would take—the code-based resilience metric assumes that the repair work can take anywhere between in the magnitude of  $10^0$ – $10^6$  s—and informs the operator how long the critical loads would survive. The operator would then be assisted by historical information about most likely outage duration for such events, and typical load demands, and thus choose the most optimum control action. Since the code-based metric can inform the survivability of the grid across a large time scale of outage durations, it provides the operator with unique flexibility to take aggressive or conservative control actions, and subsequently change or optimize the control actions to better suit the network needs, if deemed necessary.

Let us demonstrate the computation of each constituent variable of  $R$ , by considering a generic variable  $m$ , to compute the resilience of a network lasting to an event lasting  $\alpha$  s. We propose an empirical equation for unscaled resilience metric as

$$m' = c(\alpha + e^f)(1 + f) \quad (2)$$

where  $m'$  is the unscaled value of the resilience value,  $c$  is a binary variable, which stores whether an event happened in the considered time frame, and  $f$  is the fraction of load unaffected by the PDS event, determined from (1). Equation (3) is formulated because resilience of a PDS is proportional to the time duration of impact it can sustain, and the fraction of loads unaffected because of the event in the network. The fraction of loads (or any other factor representing the network infrastructure) that remains intact after a contingency is represented as an exponential function. The term  $(1 + f)$  has been used to denote the proportionality of the resilience metric to the fraction of unaffected loads.  $(1 + f)$  is used instead of  $f$  to make the resiliency metric scale from one to nine.

Each constituent factor used to represent  $R$  is a function of time duration of the impact as well as  $m'$ , which itself is another function of time duration of outage  $\alpha$ , and dependent proportionally and exponentially on a fraction of unaffected loads. It can be observed from (2) that the fraction of unaffected load affects the value of resilience significantly, and time scale of the event is captured through the range of  $\alpha$ . In case of a detected PDS event, the most resilient systems will have

$$m'_{\max} = (\alpha_{\max} + e^1)(1 + 1) = 25.41 \quad (3)$$

$$m'_{\min} = (\alpha_{\min} + e^{0+}) = 1. \quad (4)$$

The unscaled  $m'$  maximum and minimum resilience values are resolved to an integer value  $m$  between 1 and 9 (1 for least resilient and 9 for most resilient), as shown in Table I. If  $f = 0$ ,  $m$  is forced to store 1. Any case of no event affecting the PDS in the order of  $10^n$  s under evaluation,  $m$  is represented as

0. In (4),  $f = 0+$  is used instead of 0 for the most resilient state of the PDS. Otherwise, it would be impossible to distinguish an unfavorable event from nonoccurrence of any unfavorable event in the PDS.

1) *Example*: Consider that a transient surge affects two-thirds of entire PDS customer demand for  $6.12 \times 10^3$  s. However, since the event lasts  $10^3$  s, we have to calculate  $C$ . Using (2),  $C' = 1(6.12 + e^{0.333})(1 + 0.333) = 10.01$ . From Table I,  $C$  is resolved to be 4. In a second event, if only one-third of the PDS customer demand is affected for the same duration due to a transient surge,  $C' = 1(6.12 + e^{0.667})(1 + 0.667) = 13.44$ . From Table I,  $C$  is resolved to be 5. Thus, we can clearly see the improvement in resilience due to greater percentage of unaffected loads.

Let us assume that for a utility PDS, the resilience metric has been determined to be  $R_1 = 112\ 578$ . It means that distribution system has low resilience to outages lasting in order to  $10^4$ – $10^6$  s, but moderate to high resilience to outages lasting  $10^3$ – $10^1$  s. If another PDS is to be compared, or another configuration of the same PDS is evaluated for resilience using the proposed method, let us say  $R_2 = 113\ 689$ . The new metric shows that the resilience in continuity of service in the second PDS is higher for events lasting in order of  $10^1$ – $10^4$  s, but the resilience to power quality events in the power system has declined. The change in resilience could be computed as  $\Delta(R_1 - R_2)$ , which is computed using the following equation:

$$\begin{aligned} \Delta R_1 - R_2 = & (A_1 - A_2) 10^6 (B_1 - B_2) 10^5 (C_1 \\ & - C_2) 10^4 (D_1 - D_2) 10^3 (E_1 \\ & - E_2) 10^2 (F_1 - F_2) 10^1. \end{aligned} \quad (4a)$$

2) *Example of Computing Difference in Resilience Between Two Operating States,  $R_1$  and  $R_2$* : If  $R_1$ , measured during an operating state, is equal to 188, and  $R_2$  is the measured resiliency state after some switching operation, or addition of distributed generator, then  $\Delta(R_1 - R_2)$  would be indicative of the improved resilience of the network. In other words, 203–188 would imply that the resiliency improved from 3 to 8 for an event that typically lasts in the order of  $10^1$  s, 0 to 8 for an event that typically lasts in the order of  $10^2$  s, and deteriorated from 2 to 1 for an event that typically lasts in the order of  $10^3$  s. We have added a similar example, as suggested by the reviewer, in this paper to clearly suggest how change in resilience in the proposed code-based metric is to be interpreted.

Evaluating the resilience of a PDS is challenging because multiple noncommensurate factors determine the resilience of a network. A variety of tools are used to enable the resilience of a PDS, such as advanced DMS algorithms based on artificial intelligence and devices such as smart switches, reclosers, fault-detection and isolation devices, auto-transfer switches, onsite distributed generation (diesel, natural gas, and renewables), and battery storage. However, without a real-time resilience evaluation framework for quantification, it is not possible to gauge the effectiveness of the resilience-enhancement method adopted by the utility.

The essential difference between using the proposed code-based metric and computing resiliency over time is as follows.

- 1) The code-based metric is derived by computing the resilience of the network several times for all possible outage durations, and not all possible outage scenarios (which may be done by computing all the possible edges in which an overhead line can be damaged). On the other hand, any other resiliency metric may be computed on several possible outage scenarios and putting them together coherently will result in a large look-up table. However, the code-based metric is concise (six digits) and conveys information about system resilience over a large time scale conveniently.
- 2) The code-based metric is a temporal representation of resilience, and abstracts the availability of infrastructure and associated probabilistic parameters in the representation. Thus, it can quickly provide approximate losses to be incurred in terms of Energy Not Served (or utility revenue lost by multiplying by the cost per kilowatt-hour), unlike other resilience metrics that can be computed by combinatorial investigation of all possible failures specific to and eventually collated. Since the proposed metrics considers encoding the network resilience upon time taken to restore the network, it makes the proposed resilience metric representation universal and easy to compare different distribution networks with diverse capacities and priorities. For example, if an operator reports that the resilience metric of Network A is “114 899” and another operator of Network B says that the resilience of Network B is “135 999,” it clearly implies that Network B is more resilient to Network A for outages lasting in the scale of  $10^3$  s.

### III. DYNAMIC ADJUSTMENT OF OPERATING CONDITION TO MAXIMIZE RESILIENCY

Dynamic optimization of operating criteria is required to ensure maximum sustainability of limited resources after a contingency. Many authors have proposed that resiliency be enabled by only keeping the critical loads on during the contingency. In the simplest sense, the operating curve of a distribution system can be represented by Curve A' in Fig. 2, where  $E_{\text{stored}}$  represents the backup energy available in the system at the time of contingency. The most commonly used utility practice includes shedding a certain fraction of load and continue to supply the residual grid until power is restored, or the grid under contingency runs out of power. Curve A shows an ideal response in which the power grid can completely maintain all loads until the outage inducing event has been overcome. Curves B and C show different approaches that can be adopted for power consumption when the grid is in an islanded mode. Curve B shows exponential decay, in which the energy supplied any of the critical loads will not be able to meet the energy demand over the duration of the outage. Curve C shows the benefit of dynamic optimization based operating practice that ensures high sustainability of resources that out lasts duration of the outage.

Under ideal circumstances, the time for which the secondary resources should be available to feed the critical loads (i.e.,  $t_{\text{backup}}$ ) should equal or be more than  $t_{\text{restored}}$ . However, in many practical scenarios,  $t_{\text{backup}} < t_{\text{restored}}$ , necessitating further investigation into dynamic optimization of operating set-points such that maximum load is picked up, for the maximum amount of time.

The resilient energy requirement of the grid may be written as

$$E^{\text{reqd}} = \int_{t_{\text{event}}}^{t_{\text{repair}}} P_{\text{crit}}(t) dt. \quad (5)$$

The energy available for a grid that is undergoing a contingent situation is given by

$$E^{\text{avail}} = \sum_{1 \rightarrow g} \int_{t_{\text{event}}}^{t_{\text{outage}}} P_{\text{gen}}(t) dt + \sum_{1 \rightarrow b} \int_{t_{\text{event}}}^{t_{\text{outage}}} P_{\text{batt}}(t) dt \quad (6)$$

where  $g$  is the number of generators in the microgrid,  $b$  is the number of battery installations in the microgrid,  $P_{\text{gen}}$  is the power delivered from individual diesel generators, and  $P_{\text{batt}}$  is the power delivered from batteries. The power delivered by the generator and the battery can be modeled using the following equations:

$$P_{\text{gen}} = \begin{cases} P_0 e^{r_1 \tau_1} & t_{\text{event}} < t < t_{\text{steady}} \\ \eta P_{\text{rated}} & t_{\text{steady}} < t_{\text{fuel}} \\ 0 & t_{\text{fuel}} < t_{\text{repair}} \end{cases} \quad (7)$$

$$P_{\text{batt}} = \begin{cases} \eta_{\text{batt}} P_{\text{rated}} & t_{\text{outage}} < t_{\text{SOC}} \\ \eta_{\text{batt}} P_{\text{rated}} e^{-r_2 \tau_2} & t_{\text{SOC}} \leq t_{\text{repair}} \end{cases} \quad (8)$$

where  $\tau_1$  is the time constant of the generator to reach steady-state rated power generation capacity after being brought online,  $\tau_2$  is the time constant of the power availability decay curve of the battery after it threshold state-of-charge required for constant power delivery is reached,  $r_1$  is the rate at which power ramping rate of the diesel generator,  $r_2$  is the power decay rate of the battery, and  $t_{\text{fuel}}$  is the time at which fuel supply of the generator falls below critical values. The time taken for a battery to be discharged to a level beyond which it fails to act as a constant power source is represented by  $t_{\text{SOC}}$ . It may be recalled that  $r_1 = Ap^2 + Bp + C$  corresponds to the fuel consumption curve of the generators, where  $A$ ,  $B$ , and  $C$  correspond to specific parameters of a generator.

Assuming less than ideal industrial operating conditions, let us define an energy deficit optimization function such as

$$\begin{aligned} \min E^{\text{deficit}} &= aE^{\text{reqd}} - bE^{\text{avail}}(r_1, r_2) \\ \text{s.t.} \quad &\begin{cases} 0 \leq a \leq 1.0 \\ -\infty < b < +\infty \\ r_{1\min} \leq r_1 \leq r_{1\max} \\ r_{2\min} \leq r_2 \leq r_{2\max} \end{cases} \end{aligned}$$

where  $a$ ,  $b$  are adjustable parameters of the deficit function.

A linear programming model is created to optimize the use of limited resources available to serve the most important loads for the longest duration of time during a contingency to maximize the resilience of the grid.

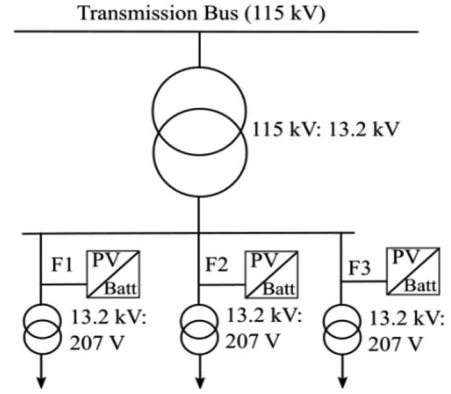


Fig. 5. Simple PDS.

#### A. Application of Dynamic Adjustment of Operating Conditions

Since distribution systems serve communities, some loads, such as those committed for law enforcement and public service, are higher priority loads compared to residential loads. Thus, if not already available, it is relatively expensive to create load priority lists for all distribution systems. At the discretion of the operator, loads are labeled “High Priority,” others are classified as “Medium Priority” or “Low Priority.” Among each of these categories, further subdivisions are possible—though such sophisticated classification is less than practical. During contingencies, it is practical to continually monitor the situation and evolve the operating set-points. The dynamic optimization problem requires the estimated time left to repair, and optimizes the fuel consumption rate of diesel generators and the connected critical loads, so as to maximize the time for which the most critical load can be served.

---

#### Algorithm 1: Dynamic Adjustment of Operating Conditions for Longer Service of Most Critical Load.

---

Input:  $t_{\text{repair}}$ ,  $P_{\text{gen}}$ ,  $P_{\text{batt}}$ ,  $\eta_{\text{gen}}$ ,  $\eta_{\text{batt}}$

Output:  $a$ ,  $b$ ,  $r_1$ , and  $r_2$

Initial Conditions:  $a \leftarrow a^{\text{init}}$ ,  $b \leftarrow 1$ ,  $r_1 \leftarrow r^{\text{init}}$

- 1:  $E^{\text{reqd}} \leftarrow$  Compute energy required
  - 2:  $E^{\text{avail}} \leftarrow$  Compute available energy
  - 3:  $E^{\text{deficit}} \leftarrow$  Compute energy deficit at start of the event
  - 4: **while**  $E^{\text{deficit}} > 0$  :
    - 5: Run Linear Programming
    - 6: Reduce  $r_1$ ,  $b^{\text{optimal}} \rightarrow b^{\text{new}}$
    - 7: Forward-Backward Power flow to check for convergence
    - 8: **if**  $\text{convergence} = \text{true}$ :
      - 9: Compute  $E^{\text{deficit}}$
    - 10: **End while**
    - 11: **else**: reset to initial conditions
    - 12: **End while**
- 

#### B. Relationship with Proposed Resiliency Metric

The proposed code-based resiliency metric is inadequate to quantify and compare the impact of unfavorable events that last

TABLE II  
RESILIENCY METRICS OF SIMPLE SYSTEM CASE STUDY

Duration of event (s)	Affected loads in simulation scenario	Code	With no PV, but only battery		With PV and battery	
			Resiliency value (m)	Scaled value ( $R_1$ )	Resiliency value	Scaled value ( $R_2$ )
$10^6$	Feeder 1, Feeder 2, Feeder 3 [Simulation method: Disconnected from the utility for indeterminate time]	A	1.67	1	6.53	3
$10^5$	Feeder 1, Feeder 2, Feeder 3 (Simulation method: trip breaker on Feeder 3 and eliminate the section for subsequent simulations)	B	1.86	1	23.78	9
$10^4$	Feeder 2, Feeder 3 (Simulation method: trip breaker on Feeder 3)	C	23.78	9	23.78	9
$10^3$	Feeder 1, Feeder 2, Feeder 3 (Simulation method: disconnection of all feeders from substation)	D	18.56	7	23.78	9
$10^2$	Feeder 3 (Simulation method: timed disconnection and reconnection to PDS of feeder 3 load – battery brought online immediately after disconnection from utility)	E	1.00	1	21.84	8
$10^1$	Feeder 3 (Simulation method: Rapid application and clearing of fault within few cycles)	F	1.67	1	1.67	1

in the order of  $10^4$  to  $10^6$  seconds on several networks, because for most networks the value is close to 1 for such long duration events. The dynamic optimization of operating conditions is aimed at increasing the sustainability of the most critical load in a distribution grid, and thereby the resiliency of the grid to unfavorable events that last in the order than  $10^4$  to  $10^6$  seconds. Dynamic optimization of the operating criteria of the energy resources in the islanded grid is suitable for formally studying the impact of time-intensive forced repairs on the power grid.

#### IV. SIMULATION RESULTS & CASE STUDIES

##### A. Simple One-Substation, Three Load Case Study

The proposed resiliency evaluation approach of a distribution network is demonstrated on a PDS using MATLAB/Simulink (shown in Fig. 5). Solar power generation (maximum 5 kW) is a renewable energy source. Power sources are system power, solar power generation, and a storage battery (150 V, 30 A·h). The storage battery is controlled by a battery controller, and it absorbs surplus power (if there is surplus power in the PDS) or it supplies insufficient power (if there is a power deficit in the PDS). Three Feeders consume power (2.5 kW peak load) as electric loads.

##### B. Simulation Results of Simple System

In assumed load profile, from 8 P.M. to 4 A.M., solar power generation is 0 W. It reaches the peak amount (5 kW) between 2 P.M. and 3 P.M. As a typical load change in ordinary feeders, the amount of electric power load reaches peak consumption at 9 (6500 W), 19, and 22 h (7500 W). From midnight until noon

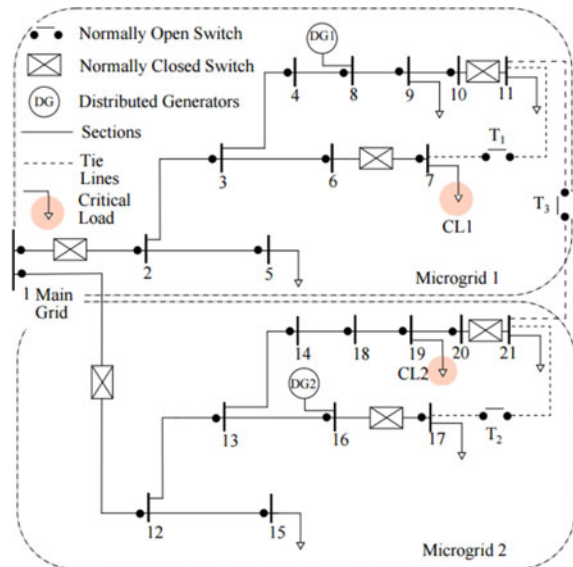


Fig. 6. Multiple CERTS microgrid systems connected to same substation.

and from 6 P.M. until midnight, battery control is performed by a battery controller. The battery control performs tracking control of the current so that active power, which flows into system power from the secondary side of the pole transformer, is set to 0. Then, the active power of secondary side of the pole-mounted transformer is always around zero. The storage battery supplies the insufficient current when the power of the PDS is insufficient and absorbs surplus current from the PDS when its power surpasses the electric load. From noon until 6 P.M., battery



TABLE III  
RESILIENCE QUANTIFICATION IN MODIFIED CERTS MULTIPLE MICROGRID WITH DIESEL GENERATOR POWER BACKUP

Duration of event (s)	Affected critical loads in simulation scenario	Code	With PV/battery-based distributed generation (day-time, peak load)		With PV/battery-based distributed generation (night-time average load)	
			Resilience value (m)	Scaled value ( $R_1$ )	Resilience value	Scaled value ( $R_2$ )
$10^6$	CL1, CL2 scenario: Islanded from the grid due to transmission line problems	A	16.89	<b>6</b>	11.23	<b>4</b>
$10^5$	CL1, CL2 scenario: Triple line to ground fault in Section 1–2	B	22.91	<b>9</b>	14.46	<b>6</b>
$10^4$	CL1, CL2 scenario: Single line to ground fault in Section 3–6, and single line to ground fault in 14–18	C	24.71	<b>9</b>	24.71	<b>9</b>
$10^3$	CL2 scenario: Single line to ground fault in 14–18. Fault caused delay in loads to function again at peak, leading to increase in effective fault duration	D	23.56	<b>9</b>	23.56	<b>9</b>
$10^2$	CL1 scenario: Single line to ground fault in Section 3–6 that required resetting of relay settings	E	23.09	<b>9</b>	23.09	<b>9</b>
$10^1$	CL1, CL2 scenario: Fault in Section 1–2 cleared within 5 cycles	F	22.71	<b>9</b>	22.71	<b>9</b>

control is not performed. State of charge (SOC) of the storage battery is fixed to a constant and does not change since charge or discharge of the storage of the example PDS.

Resilience results from different PDS operating conditions are summarized in Table II. In Table II, by comparing  $R_1$  and  $R_2$ , it can be concluded that the addition of photovoltaic (PV) and battery to the PDS increases the resilience of the network to long power outage events.

### C. Simulation Results on Multiple Microgrid CERTS System

The consortium of electric reliability technology (CERTS) Microgrid concept was defined as a group of distributed generators and storage with the ability to separate and island itself from the utility grid seamlessly with minimal disruption to the connected loads. Two microgrids, located adjacent to each other (shown in Fig. 6), can be operated together to take advantage of shared resources and maintaining power to critical loads of both microgrids.

The concept of multiple microgrids (or “multimicrogrids”) was introduced by the EU MORE Microgrid projects with the objective of enhancing the resiliency of distribution systems [35].

Thus, a system that is engineered for higher reliability is a suitable system for studying quantification of resiliency. The distributed generators (DGs) have been located at nodes 8 and 16, capable of serving 165.6 kW critical load demand of the network. The remaining capacity of the generators is used to feed the remainder of the normal loads in the same feeder as critical loads. The critical loads CL1 and CL2 are identified at nodes 7 and 19, respectively, as shown in Fig. 6. There are six

normally closed sectionalizing switches, and it is possible to install three tie-lines with normally open switches (T1, T2, and T3) in network between nodes 7–11, 17–21, and 11–21. It has been assumed that a smart reconfiguration algorithm has been in the distribution system. If the restoration algorithm had not been implemented by default, the resiliency values for an events of duration  $10^1$ – $10^4$  s (i.e., events that range in seconds to several hours) would have been modified further, which is beyond the scope of this paper, and can be studied in a future work.

Several operating and fault conditions have been simulated for the multiple CERTS microgrid system. Tables IV and V summarize the fault duration and the corresponding resiliency of the system depending upon the availability of backup power resources. Since many microgrids are being designed with a focus on high penetration of renewable energy resources, all the DGs shown in Fig. 3 have been studied as both conventional diesel generators and PV panels are integrated with battery storage. The PV and battery models are the same as in [36], and are modified to be of equal rating as the diesel generator DGs. The differences in resiliency value in systems with only diesel DG and systems with PV are computed by comparing corresponding columns in Tables III and IV.

Tables III and IV shows the simulation results for resiliency values in different operating conditions for CERTS microgrid. It can be observed that the proposed approach effectively captures the ability of a system to maintain acceptable performance, during potential outages that can last from seconds to several days. For outages lasting a few hours, gas-fired DGs show significantly higher resiliency; however, if such DGs are replaced with solar PV modules of equivalent capacity, the resiliency in such systems is higher during outage for longer durations.



TABLE IV  
RESILIENCE QUANTIFICATION IN MODIFIED CERTS MULTIPLE MICROGRID WITH PV-DISTRIBUTED GENERATION

Duration of event (s)	Affected critical loads in simulation scenario	Code	With no distributed generation or battery backup in any load		With nonrenewable diesel generator distributed generation	
			Resilience value (m)	Scaled value ( $R_1$ )	Resilience value	Scaled value ( $R_2$ )
$10^6$	CL1, CL2 scenario: Islanded from the grid due to transmission line problems	A	1.07	<b>1</b>	11.03	<b>4</b>
$10^5$	CL1, CL2 scenario: Triple line to ground fault in Section 1–2	B	1.43	<b>1</b>	13.73	<b>5</b>
$10^4$	CL1, CL2 scenario: Single line to ground fault in Section 3–6, and single line to ground fault in 14–18	C	1.43	<b>1</b>	24.71	<b>9</b>
$10^3$	CL2 scenario: Single line to ground fault in 14–18. Fault caused delay in loads to function again at peak, leading to increase in effective fault duration	D	1.43	<b>1</b>	23.56	<b>9</b>
$10^2$	CL1 scenario: Single Line to Ground Fault in Section 3–6 that required resetting of relay settings	E	1.43	<b>1</b>	23.09	<b>9</b>
$10^1$	CL1, CL2 scenario: Fault in Section 1–2 cleared within 5 cycles	F	22.71	<b>9</b>	22.71	<b>9</b>

TABLE V  
RESILIENCY METRICS WITH AND WITHOUT DYNAMIC OPTIMIZATION IN MODIFIED CERTS MICROGRID

Operating scenario	With optimization	Without optimization (only $b$ )	With optimization ( $b$ and $r_1$ )
With PV and Diesel DG	789 999	699 999	799 999
With only Diesel DG and No PV	689 999	469 999	589 999

#### D. Dynamic Optimization of Resilient Operating Conditions

In this scenario, the CERTS system with similar PV and diesel DGs are used. It has been assumed that 80% of the critical loads of the network have been classified as the high-priority loads among the critical loads. Three scenarios are simulated. In the first scenario, the dynamic optimization of resources is not implemented. It was observed that for events lasting multiple days ( $10^6$  s), none of the critical load could be survived. However, if only the fraction of critical load kept alive could be optimized, higher amounts of critical loads could be kept on for events lasting several hours ( $10^4$  and  $10^5$  events). Without optimization, only 17.461% of critical loads can be maintained for an event lasting more than a day (about 27 h). However, implementing the optimization fraction of critical load, the 23.191% of critical loads could remain online. When the optimization algorithm was used to optimize the synthetic aggregated fuel curve of the DGs, the 4.251% critical load could survive an outage lasting 11 days. The results have been summarized in Table V, and the interpolated plots of event duration versus fraction of critical load served are been shown in Fig. 7.

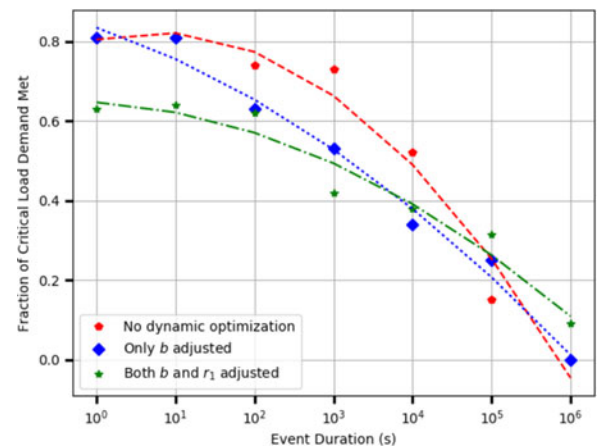


Fig. 7. Impact of dynamic optimization for very long duration outages.

#### V. CONCLUSION

This paper presents a novel and feasible framework for quantifying, monitoring, and leveraging resilience metrics of PDS. A comprehensible and comprehensive metric has been developed, which provides insights into the impact of contingencies across a broad spectrum of events. An advantage of such a metric is that it can be implemented in field using existing tools and with no learning curve for operators. It is important to highlight that the primary use of the metric is to convey the impact of an event to an operator or engineer in real time. When a contingent event occurs, the repair/restoration duration is not known. In many occasions, repair work done to restore the system to precontingency state is very quickly followed by a subsequent attack

or event that may lead to loss of power of the restored critical loads. The metric computation algorithm quantifies the ability of the network to sustain normal functionality of the critical load for a broad range of times in a single computation step, from a few seconds to a week. In a future work, the proposed algorithm can be formally investigated and developed using parallel computation techniques to increase the computation efficiency. A metric that quantifies the resilience of the system over a wide time scale—by appending several calculations into a single observable quantity—provides a broader perspective to the overall resilience of the network.

The developed metrics formulation quantifies the ability of the system to supply critical loads with reduced resources. Though the metrics have been developed for electric utility and power system, the metrics can be generalized to any flow networks. Based on resilience values under several operating and planning scenarios, cost–benefit analysis of distribution system investments can be justified. A dynamic optimization algorithm that progressively reduces amount of critical load served to maximize the sustainability of most critical load is proposed. This optimization when integrated into the resiliency metric can be implemented to maximize the duration for which the most important load in a microgrid can be sustained. The information derived from the proposed resilience metric can be used to design PDS to serve consumers with higher reliability. The proposed time-dependent resilience metric is scalable to different PDS topologies, preserves diverse noncommensurate information, and easily interpretable by operators. The proposed optimization algorithm can be further improved in a future work by improving the parameter identification of the factors that influence the duration for which the most critical load can be provided, such as fuel cost curve, generator, and battery ramp up and down rates.

## REFERENCES

- [1] H. H. Willis and K. Loa, "Measuring the resilience of energy distribution systems," RAND Corporation, Santa Monica, CA, USA, Res. Rep. RR-883-DOE, 2015.
- [2] S. Chanda and A. K. Srivastava, "Quantifying resiliency of smart power distribution systems with distributed energy resources," in *Proc. IEEE 24th Int. Symp. Ind. Electron.*, 2015, pp. 766–771.
- [3] M. J. Sullivan, "Interruption costs, customer satisfaction and expectations for service reliability," *IEEE Trans. Power Syst.*, vol. 11, no. 2, pp. 989–995, May 1996.
- [4] X. Liu, M. Shahidehpour, Z. Li, X. Liu, Y. Cao, and Z. Bie, "Microgrids for enhancing the power grid resilience in extreme conditions," *IEEE Trans. Smart Grid*, vol. 8, no. 2, pp. 589–597, Mar. 2017.
- [5] G. Jiménez-Estévez, A. Navarro-Espinosa, R. Palma-Behnke, L. Lanuzza, and N. Velázquez, "Achieving resilience at distribution level: Learning from isolated community microgrids," *IEEE Power Energy Mag.*, vol. 15, no. 3, pp. 64–73, May/Jun. 2017.
- [6] H. Gao, Y. Chen, S. Mei, S. Huang, and Y. Xu, "Resilience-oriented pre-hurricane resource allocation in distribution systems considering electric buses," in *Proc. IEEE*, vol. 105, no. 7, pp. 1214–1233, Jul. 2017.
- [7] A. Khodaei, "Provisional microgrids," *IEEE Trans. Smart Grid*, vol. 6, no. 3, pp. 1107–1115, May 2015.
- [8] S. Lei, J. Wang, C. Chen, and Y. Hou, "Mobile emergency generator pre-positioning and real-time allocation for resilient response to natural disasters," *IEEE Trans. Smart Grid*, to be published, doi: [10.1109/TSG.2016.2605692](https://doi.org/10.1109/TSG.2016.2605692).
- [9] M. Simonov, "Dynamic partitioning of DC microgrid in resilient clusters using event-driven approach," *IEEE Trans. Smart Grid*, vol. 5, no. 5, pp. 2618–2625, Sep. 2014.
- [10] Z. Wang and J. Wang, "Self-healing resilient distribution systems based on sectionalization into microgrids," *IEEE Trans. Power Syst.*, vol. 30, no. 6, pp. 3139–3149, Nov. 2015.
- [11] A. Khodaei, "Resiliency-oriented microgrid optimal scheduling," *IEEE Trans. Smart Grid*, vol. 5, no. 4, pp. 1584–1591, Jul. 2014.
- [12] A. Gholami, T. Shekari, F. Aminifar, and M. Shahidehpour, "Microgrid scheduling with uncertainty: The quest for resilience," *IEEE Trans. Smart Grid*, vol. 7, no. 6, pp. 2849–2858, Nov. 2016.
- [13] H. Farzin, M. Fotuhi-Firuzabad, and M. Moeini-Aghaie, "Enhancing power system resilience through hierarchical outage management in multi-microgrids," *IEEE Trans. Smart Grid*, vol. 7, no. 6, pp. 2869–2879, Nov. 2016.
- [14] S. Arianos, E. Bompard, A. Carbone, and F. Xue, "Power grids vulnerability: A complex network approach," *Chaos*, vol. 19, 2009, Art. no. 013119.
- [15] P. Bajpai, S. Chanda, and A. K. Srivastava, "A novel metric to quantify and enable resilient distribution system using graph theory and Choquet integral," *IEEE Trans. Smart Grid*, to be published, doi: [10.1109/TSG.2016.2623818](https://doi.org/10.1109/TSG.2016.2623818).
- [16] H. K. LaCommare and J. H. Eto, "Understanding the cost of power interruptions to US electricity consumers," Lawrence Berkeley Nat. Lab., Berkeley, CA, USA, Tech. Rep. 55718, 2004.
- [17] F. O. Resende, N. J. Gil, and J. A. P. Lopes, "Service restoration on distribution systems using multi-microgrids," *Eur. Trans. Elect. Power*, vol. 21, no. 2, pp. 1327–1342, Mar. 2011.
- [18] T. Shekari, F. Aminifar, and M. Sanaye-Pasand, "An analytical adaptive load shedding scheme against severe combinational disturbances," *IEEE Trans. Power Syst.*, vol. 31, no. 5, pp. 4135–4143, Sep. 2016.
- [19] S. Chanda and A. K. Srivastava, "Defining and enabling resiliency of electric distribution systems with multiple microgrids," *IEEE Trans. Smart Grid*, vol. 7, no. 6, pp. 2859–2868, Nov. 2016.
- [20] S. Chanda, "Measuring and enabling resiliency in distribution systems with multiple microgrids," M.S. thesis, Dept. School Elect. Eng. Computer Sci., Washington State Univ., Pullman, WA, USA, 2015.
- [21] M. De Nooij, C. Koopmans, and C. Bijvoet, "The value of supply security: The costs of power interruptions: Economic input for damage reduction and investment in networks," *Energy Econ.*, vol. 29, no. 2, pp. 277–295, 2007.
- [22] R. V. Solé, M. Rosas-Casals, B. Corominas-Murtra, and S. Valverde, "Robustness of the European power grids under intentional attack," *Phys. Rev. E*, vol. 77 no. 2, 2008, Art. no. 026102.
- [23] L. Lawton, M. Sullivan, K. Van Liere, A. Katz, and J. Eto, "A framework and review of customer outage costs: Integration and analysis of electric utility outage cost surveys," Lawrence Berkeley Nat. Lab., Berkeley, CA, USA, Tech. Rep. LBNL 54365, 2003.
- [24] Y. Wang, C. Chen, J. Wang, and R. Baldick, "Research on resilience of power systems under natural disasters—A review," *IEEE Trans. Power Syst.*, vol. 31, no. 2, pp. 1604–1613, Mar. 2016.
- [25] C. Ji, Y. Wei, and H. V. Poor, "Resilience of energy infrastructure and services: Modeling, data analytics, and metrics," *Proc. IEEE*, vol. 105, no. 7, pp. 1354–1366, Jul. 2017.
- [26] E. C. Venizelos, D. N. Trakas, and N. D. Hatziaargyriou, "Distribution system resilience enhancement under disastrous conditions by splitting into self-sufficient microgrids," in *Proc. IEEE Manchester PowerTech Conf.*, Manchester, U.K., 2017, pp. 1–6.
- [27] A. Rose, G. Oladosu, and S.-Y. Liao, "Business interruption impacts of a terrorist attack on the electric power system of Los Angeles: Customer resilience to a total blackout," *Risk Anal.*, vol. 27, no. 3, pp. 513–531, 2007.
- [28] S. Chanda, A. K. Srivastava, M. U. Mohanpurkar, and R. Hovsapien, "Quantifying power distribution system resiliency using code based metric," in *Proc. 2016 IEEE Int. Conf. Power Electron., Drives, Energy Syst.*, Trivandrum, India, pp. 1–6, doi: [10.1109/PEDES.2016.7914553](https://doi.org/10.1109/PEDES.2016.7914553).
- [29] E. D. Vugrin, D. E. Warren, M. A. Ehlen, "A framework for assessing the resilience of infrastructure and economic systems," in *Sustainable and Resilient Critical Infrastructure Systems*, K. Gopalakrishnan, S. Peeta Eds. Berlin, Germany: Springer, 2010, pp. 77–116.
- [30] M. Panteli and P. Mancarella, "Influence of extreme weather and climate change on the resilience of power systems: Impacts and possible mitigation strategies," *Elect. Power Syst. Res.*, vol. 127, pp. 259–270, 2015.
- [31] J. Watson *et al.*, "Conceptual framework for developing resilience metrics for the electricity, oil, and gas sectors in the United States," Sandia Nat. Lab., Albuquerque, NM, USA, Tech. Rep. 18019, 2015.
- [32] T. Kropp, "System threats and vulnerabilities [power system protection]," *IEEE Power Energy Mag.*, vol. 4, no. 2, pp. 46–50, Mar./Apr. 2006.

- [33] S. M. Amin and B. F. Wollenberg, "Toward a smart grid: Power delivery for the 21st century," *IEEE Power Energy Mag.*, vol. 3, no. 5, pp. 34–41, Sep./Oct. 2005.
- [34] Z. Zeng, H. Yang, S. Tang, and R. Zhao, "Objective-oriented power quality compensation of multifunctional grid-tied inverters and its application in microgrids," *IEEE Trans. Power Electron.*, vol. 30, no. 3, pp. 1255–1265, Mar. 2015.
- [35] N. Hatziaargyriou, H. Asano, R. Iravani, and C. Marnay, "Microgrids," *IEEE Power Energy Mag.*, vol. 5, no. 4, pp. 78–94, Jul./Aug. 2007.
- [36] J. Copetti, E. Lorenzo, and F. Chenlo, "A general battery model for PV system simulation," *Prog. Photovolt.: Res. Appl.*, vol. 1, no. 4, pp. 283–292, 1993.



**Sayonsom Chanda** (S'13) received the master's degree in electrical engineering from Washington State University, Pullman, WA, USA, in 2015, where he is currently working toward the Ph.D. degree.

He worked as a Research Engineer in the Energy Storage and Transportation Systems Department, Idaho National Laboratory, Idaho Falls, ID, USA. His research interests include reliability and resiliency of power distribution systems, complex network analytics, and integration of energy systems devices for power grid applications.

He is a registered Engineer-in-Training in the state of ID, USA.



**Anurag K. Srivastava** (SM'09) received the Ph.D. degree in electrical engineering from the Illinois Institute of Technology, Chicago, IL, USA, in 2005.

He worked as an Associate Professor at Washington State University, Pullman, WA, USA. His research interests include power system operation and control, synchrophasors applications, microgrid resiliency, and cyber-physical analysis of power system.

Dr. Srivastava is an Associate Editor for the IEEE TRANSACTIONS ON SMART GRID and the IEEE

TRANSACTIONS ON POWER SYSTEMS, and as an IEEE Distinguished Lecturer.



**Manish U. Mohanpurkar** (M'14) received the M.S. degree from Oklahoma State University, Stillwater, OK, USA, and the Ph.D. degree from Colorado State University, Fort Collins, CO, USA, in 2010 and 2013, respectively.

He is currently working as a Group Lead with the Idaho National Laboratory, Idaho Falls, ID, USA, and works broadly in the area of power and energy systems. He has more than 10 years of research experience in power systems analysis, probabilistic and steady-state analysis, real-time digital simulation, hardware-in-the-loop, dynamic and transient analysis, power markets, assimilation of renewable energy, and energy resource planning studies. His past research was related to wind energy, hydro-electric power generation, and energy-storage technologies such as pumped storage hydro, electrolyzers, microgrids, and electric vehicles. He has more than 30 publications in leading power- and energy-related venues.



**Rob Hovsapien** (SM'02) received the B.S. degree from the University of Alabama, Tuscaloosa, AL, USA, in 1986, and the M.S. and Ph.D. degrees from Florida State University, Tallahassee, FL, USA, 1988 and 2009, respectively.

He is an Energy Systems Scientist with experience in system-level modeling of energy systems. He is currently working as a Department Manager with the Idaho National Laboratory, Idaho Falls, ID, USA.

He is a member of the American Society of Mechanical Engineers, the American Society for Engineering Education, and Engineers Without Borders.